

Investigation Of Wind Turbine Static Yaw Error Based On Utility-Scale Controlled Experiments

Davide Astolfi, *Member, IEEE*, Fabrizio De Caro, *Member, IEEE*, Marco Pasetti, *Member, IEEE* Linyue Gao, Ravi Pandit, Alfredo Vaccaro, *Senior Member, IEEE*, Jiarong Hong

Abstract—Wind energy represents a promising alternative to replace traditional fossil-based energy sources. For this reason, increasing the efficiency in the conversion process from wind to electrical energy is crucial. Unfortunately, the presence of systematic errors (mostly related to the yaw and pitch angles) is one of the key factors causing under-performance, and for this reason, it requires adequate identification. The present work deals with diagnosing wind turbine static yaw error, occurring when the wind vane sensor is incorrectly aligned with the rotor shaft. A thorough investigation methodology is proposed by considering a unique experimental test-up shared by the Eolos Wind Research Station. A utility-scale wind turbine has been imposed to operate subjected to several static yaw errors and reference meteorological data collected nearby the wind turbine were available. By analyzing the relation between the meteorological data and the SCADA data collected by the wind turbine, a systematic alteration in the measurements of nacelle wind speed in the presence of the yaw error is explicitly shown. This phenomenon has been overlooked in the literature and leads to revisiting the methods mostly employed for the diagnosis of the error. Furthermore, a correlation between the presence of static error, increased blade pitch, and heightened levels of tower vibration is observed. In summary, this work provides a comprehensive characterization of the experimental evidence associated with the presence of a wind turbine static yaw error. This paves the way for more effective diagnostic techniques for wind turbine yaw errors, potentially revolutionizing data-driven maintenance strategies.

Index Terms—Wind Energy, Wind Turbines, Systematic Errors, Yaw Error, Renewable Energy Sources, Energy Systems Efficiency

I. INTRODUCTION

Wind turbines are considered a leading technology for power generation from renewable sources [1], [2], such that the European Commission has set a target that half of the electricity produced in Europe by 2050 should be produced from wind. Therefore, there is ever-growing attention towards the formulation of intelligent wind farm Operation & Maintenance strategies, to diminish energy losses and maximize the lifetime of the wind turbines. In this context, there is a great interest

D. Astolfi and M. Pasetti are with the Department of Information Engineering, University of Brescia, Brescia, Italy.

F. De Caro is with the Department of Industrial Engineering, University of Salerno, Fisciano, Italy.

L. Gao is with the Department of Mechanical Engineering, University of Colorado, Denver, U.S.

R. Pandit is with the Centre for Life-Cycle Engineering and Management, University of Cranfield, Bedford, U.K.

A. Vaccaro is with the Department of Engineering, University of Sannio, Benevento, Italy.

J. Hong is with the Mechanical Engineering & Saint Anthony Falls Laboratory, University of Minnesota, Minneapolis, U.S.

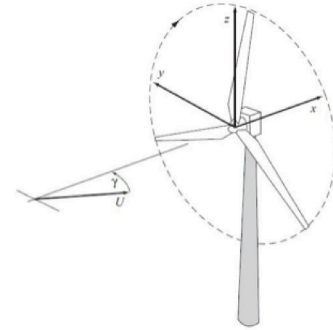


Fig. 1. Representation of a wind turbine operating subject to a static yaw error γ , adapted from [6].

in optimizing the efficiency of real-world wind turbines in operation. This objective requires reliable methods for the individuation and the solution of systematic errors affecting wind turbine operation, such as blade pitch misalignment [3], [4] and systematic yaw error [5].

The control system of a wind turbine operates to minimize the yaw error, which is represented in Fig. 1, meaning that the plane of the rotor should be perpendicular to the incoming wind. Therefore, the yaw error is generally a tempo-variable quantity that should assume a Gaussian distribution with a null mean. Due to wind vane defects, the yaw error might have also a non-vanishing static component (as in Fig. 1). In this circumstance, the control system indicates a correct alignment of the rotor although it is not perpendicular to the wind flow.

Particularly, for a static yaw error greater than 5° , the effect on the energy production starts being non-negligible [6]. Assumed a static yaw error γ , the component of the wind intensity v which is perpendicular to the rotor is $v \cos \gamma$. Since in a first approximation the extracted power P scales with the cube of the longitudinal wind intensity, a static yaw error γ affects the extracted power by a factor of $\cos^3 \gamma$. Furthermore, the presence of yaw error can affect the reliability of critical wind turbine components as the blades [7] and increases the damage-equivalent loads [8], [9].

The above considerations stimulate research to individuate the static yaw error of wind turbines [10], [11], facilitated by the widespread diffusion of Supervisory Control And Data Acquisition (SCADA) measurements, which makes available a large set of data.

Unfortunately, despite the large amount of available information, the individuation of static yaw error is challenging since the actual nacelle orientation is masked by the control

system. In other words, a wind turbine cannot be considered static yaw error-free despite the data (collected behind the rotor span) suggesting the correct alignment between nacelle orientation and wind direction. Furthermore, there are issues related to the interaction between the rotor rotation and the flow and a systematic overestimation of the wind direction deviation can be caused by the rotor misalignment [12]. Thus, several studies have been based on the use of upwind sensor systems like LiDAR [13], [14] or Spinner anemometers [15], [16]. Although the deployment of these sensors addresses the drawbacks of the SCADA-collected data, their use should be evaluated carefully due to economic considerations [17], [18].

Therefore, the literature started to develop methodologies that identify the static yaw error by employing in any case the SCADA-collected data and by analyzing the indirect consequences of the error on wind turbine operating, such as an under-performance (recall the \cos^3 law). The most relevant works are summarized in Section I-A, where the contribution of this work is outlined as well.

A. Related Work and Authors' Proposal

As above anticipated, most static yaw error diagnosis methods in the literature are based on the individuation of an under-performance. This substantially means analyzing the power curve [19], which is the relation between the incoming wind speed and the extracted power. In principle, the presence of the static yaw error should be detected from a slightly diminished extracted power for a given wind speed, although in practice the multivariate dependence of the wind turbine power advocates for non-trivial data analysis methods [20], [21].

In [22], the power curve is analyzed through the binning method upon grouping the data per yaw error intervals of 2° . In [23]–[25], the employed power curve model is Least-Square B-spline Approximation upon (similarly to [22]) grouping the data per yaw error intervals. In [26], a more complex model is employed which takes input operation variables like rotor speed and blade pitch, and the yaw error is detected from the residuals between measurements and model estimates.

Particularly, the work presented in [27] is inspiring for the present study since it is based on a reference estimate of the static yaw error provided by LiDAR measurements and includes the first critical evidence related to the power curve analysis of yaw-misaligned wind turbines. This work shows drawbacks since it analyzes the effect on the performance of the yaw static error correction by considering an experimental power curve based on the binning method, and this leads to a large, implausible, overestimation of the impact of the yaw error on the power output.

The work proposed by [28] constitutes the premise of the present study, due to the possibility of fully controlling a 2.5 MW Clipper C96 wind turbine, located at the Eolos Wind Research Station at the University of Minnesota. The authors have forced the operation of the wind turbine subjected to several values of static yaw error, thus obtaining labeled data from which they could investigate phenomena highlighting the presence of the static yaw error. In particular, the employed

method is a data-driven fit to a cosine cube law-based physical model of the power curve.

As is argued in [29] through the actuator disk model, a yaw-misaligned rotor has a different induction with respect to a well-aligned rotor. This means that the velocity deficit at the nacelle (and thus the measurement of the nacelle wind speed) for a certain incoming flow depends on the yaw error. Or, in other words, it can be argued that the presence of the static yaw error affects nacelle anemometer measurements because when a wind turbine is subjected to a static yaw error, its anemometer (which is placed behind the rotor span) will be more upwind or more downwind with respect to the case of a vanishing yaw error. Despite in this regard there is sufficient evidence in the literature (for example [29]) the state-of-the-art methods for detecting the static yaw error have notably overlooked the influence of the error on the nacelle wind speed measurements. This, for example, might explain the incoherent results collected in [27]. Only a few recent works have been taking into consideration the above issue [5], [30], which is thus notably overlooked in the literature at present.

Hence, based on the observed research gap, this paper aims to provide a comprehensive and coherent characterization of the experimental evidence associated with the presence of a wind turbine static yaw error. A distinctive aspect of this work, which makes possible to accomplish the objective, is a unique experimental test bed, which includes i) the full control for research purposes of the utility-scale wind turbine, leading to the collection of labeled data for various values of the static error; ii) the comparisons of the measurements acquired by the wind turbine through the SCADA system with data not affected by static yaw error, which are provided by a meteorological tower placed in the close area.

In particular, in this work, it is made explicit that the static yaw error influences the wind speed measurements collected by the wind turbine. This evidence has been matured by analyzing statistically the relation between the meteorological mast data and the wind turbine data for the various values of considered static yaw errors (0° , $+10^\circ$ and -10°). This result not only leads to revisiting the diagnosis methods based on the power curve but also opens new research directions because, if the static yaw error affects the wind speed measurements, such a change can be used for the diagnosis of the error.

Further experimental evidences related to the presence of the static yaw error are collected, which are variations in the blade pitch control and increased level of tower vibrations. Such evidences have not been discussed in detail in the literature before and, thus, might stimulate new research directions in the field of static yaw error diagnosis.

The manuscript, which is an extension of the conference paper [31], is organized as follows: Section II describes the experimental setup, Section III illustrates the proposed methodology, Section IV shows the obtained results, whereas Section V highlights the main conclusions.

II. THE EXPERIMENTAL SETUP

A. The Eolos Wind Research Station

The experimental facility is described in detail in [32] and we refer to that study for further information. The station

consists of a 2.5 MW upwind, 3-bladed, horizontal-axis wind turbine (Clipper Liberty C96) and a 130 m meteorological tower, sited 170 meters south of the wind turbine. A sketch of the facility is provided in Fig. 2. Four high-resolution sonic anemometers (Campbell Scientific, CSAT3, with instrumental uncertainty of 1 mm s^{-1}) are sited on the tower at meaningful heights: rotor top tip (129 m), hub height (80 m), rotor bottom tip (30 m), and standard 10 m. Cup anemometers (Met One, 014-A, with instrumental uncertainty of 0.11 m s^{-1}) are installed 3 m below each sonic anemometer. The Eolos turbine is variable-speed, variable-pitch regulated, with a rotor diameter R 96 m and a hub height of 80 m. The cut-in, rated and cut-out wind speeds are 4, 11, and 25 m s^{-1} . The available data are collected by the Supervisory Control and Data Acquisition (SCADA) data with a sampling rate of 1 Hz. The scheme of the sensor arrangement is reported in Fig. 3, where it is indicated at what height the most important quantities employed in the following are measured.

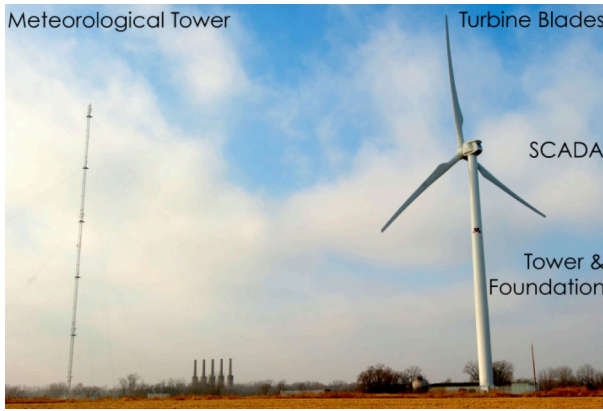


Fig. 2. The Eolos wind energy research field station including a 2.5 MW wind turbine and a 130 m tall meteorological tower.

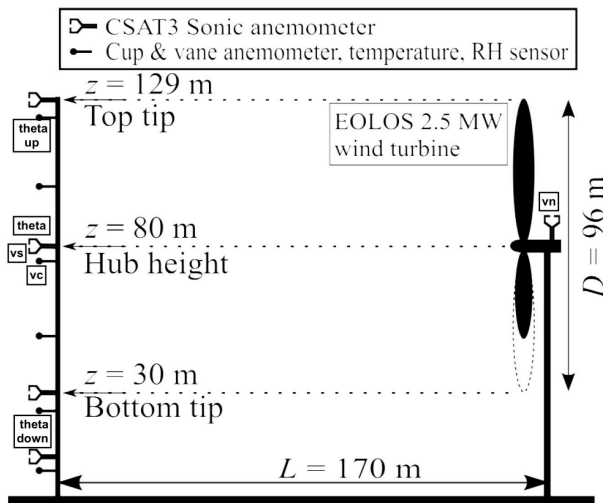


Fig. 3. The schematic illustrating the location of sonic anemometers on the meteorological and their positions with respect to the wind turbine.

The employed meteorological mast measurements are the following:

- $v_s (\text{m s}^{-1})$, wind speed measured by a sonic anemometer at the same height of the wind turbine hub (80 meters);
- $v_c (\text{m s}^{-1})$, wind speed measured by a cup anemometer placed three meters below the sonic one (i.e., 77 meters);
- $\theta_{up} (^\circ)$ is the wind direction measured at the top tip of the blade (129 meters);
- $\theta (^\circ)$ is wind direction measured at hub height;
- $\theta_{down} (^\circ)$ is the wind direction measured at the rotor bottom tip (30 meters);

whereas the employed SCADA-collected measurements are:

- $v_n (\text{m s}^{-1})$, which is the estimate of the free stream wind speed reconstructed through a nacelle transfer function (propriety of the wind farm manufacturer and thus unknown for this study) based on the measurement of the wind speed behind the rotor span from the nacelle anemometer;
- $P (\text{kW})$, which is the power output;
- $\beta (^\circ)$ is the average blade pitch;
- $\Theta (\text{m/s}^2)$ is the resultant of the tower vibrations;
- $\rho (\text{kg/m}^3)$, air density;
- turbine state.

The data analysis has been performed using Matlab 2023 with a laptop with AMD Ryzen 5 5600U with Radeon Graphics 2.30 GHz and 40 GB RAM.

B. Data sets and processing

The employed data sets are indicated in Table I. The sampling time is 1 second and the SCADA-collected data and the meteorological data are synchronized.

TABLE I
THE ANALYZED DATA SETS.

Data Set	Yaw Error	Number of samples
D_0	0°	428127
D_{10}	10°	431972
D_{-10}	-10°	518328

Particularly, the following pre-processing steps are applied:

- Data have been averaged with 10 seconds of averaging time (10 records) and their standard deviation has been computed as well;
- The turbine state must correspond to turbine “ok and running”;
- The data must be filtered on the wind direction according to the following constraint to avoid the meteorological mast being under the wake of the wind turbine: $90^\circ \leq \theta \leq 270^\circ$;
- Wind speed measurements are normalized according to (1), where $\rho_{ref} = 1.225 \text{ kg/m}^3$:

$$v_r = v \left(\frac{\rho}{\rho_{ref}} \right)^{\frac{1}{3}} \quad (1)$$

- Filter on the request in (2):

$$\Gamma = \frac{|\theta_1 - \theta_3|}{R} < 0.2^\circ/\text{m}, \quad (2)$$

where R is the rotor radius.

Particularly, (1) is a common practice to renormalize the wind speed, referring to standard air density conditions. The rationale of the filtering in (2) is selecting data with a comparable amount of wind veer [33], which is requested to be low enough to neglect the influence of such factor on rotor rotation and turbine behavior. A sensitivity analysis has been conducted on the data averaging time.

III. PROPOSED METHODOLOGY

The proposed methodology provides a comprehensive characterization of the detectable effects of the static yaw error considering several steps of analysis. In Section III-A, the relation between the wind speed measured by the meteorological mast and that measured at the wind turbine nacelle is characterized by the presence or not of the static yaw error. Consequently, the power curve analysis is revisited, as described in Section III-B. Finally, in Section III-C, data analysis methods aimed at detecting operative changes in the wind turbine (e.g. blade pitch and tower vibrations) are introduced.

A. Wind Speed Analysis

1) *Binning Curve Method*: The wind speed analysis method is based at first on visualizing the relation between the wind speed measured at the wind turbine nacelle v_n (target) and the wind speed measured at the meteorological mast v_s and v_c (references) and inquiring how this relation changes with the presence or not of the static yaw error. A qualitative assessment is achieved by employing the method of bins. It proceeds as follows:

- Group the data per intervals of the reference v_s or v_c (0.25 ms^{-1} of bin amplitude are selected, being at least twice the highest instrumental uncertainty);
- Compute the average nacelle wind speed measurements $v_{n,i}$ as in (3) for each i -th bin of meteorological mast wind speed, which will contain N_i measurements:

$$v_{n,i} = \frac{1}{N_i} \sum_{j=1}^{N_i} v_{n,ij} \quad (3)$$

where $v_{n,ij}$ is the j -th measurement of nacelle wind speed measurement comprised in the i -th bin of the reference wind speed.

- Obtain the average curves in the (v_s, v_n) or (v_c, v_n) planes, which represent the nacelle anemometer measurement v_n as a function of the met-mast measurement (sonic v_s or cup v_c).

2) *Relation Coefficients*: The relation between v_n and v_c / v_s is quantitatively assessed by considering a Monte Carlo-based approach, where the relation between the wind speed measurements is supposed to be linear ((4) and (5)). k_{ns} and k_{nc} change over different cases if an effect on wind speed measurements caused by the yaw static error is present.

$$v_n = k_{ns} v_s \quad (4)$$

$$v_n = k_{nc} v_c \quad (5)$$

For the estimation of k_{ns} and k_{nc} the Deming regression has been considered. The advantage respect with to the traditional least square models is that Deming regression considers the uncertainty of both variables.

Particularly, the coefficients k_{ns} and k_{nc} are estimated through a Montecarlo simulation as follows:

- Consider a general linear model with vanishing intercept as in (6):

$$y = ax \quad (6)$$

- Suppose that the vectors of measured x_{obs} and y_{obs} have an associated uncertainty vector σ_x and σ_y .
- Simulate the data at each Montecarlo run with (7) and (8):

$$x_{sim} = x_{obs} + \epsilon_x x_{obs} \quad (7)$$

$$y_{sim} = y_{obs} + \epsilon_y y_{obs} \quad (8)$$

where ϵ_x and ϵ_y are vectors of random numbers distributed according to standard normal distribution.

- Generate a set of N synthetic data sets. N is selected to be 500 in this study.
- Apply the Deming formulation of the least squares regression and end up with an estimate a_i for each i -th set, with $i = 1, \dots, N$;
- Compute the Montecarlo threshold as in (9):

$$\epsilon_a = \frac{2}{\sqrt{\pi}} \int_0^N e^{-t^2} dt \quad (9)$$

- Sort the vector of a_i estimates, with $i = 1, \dots, N$, in ascending order;
- Individuate the lower j_{low} and upper j_{high} index as in (10) and (11):

$$j_{low} = \lfloor N \epsilon_a \rfloor \quad (10)$$

$$j_{high} = \lceil N (1 - \epsilon_a) \rceil \quad (11)$$

- Return the Montecarlo estimates a_{est} with its uncertainty σ_a as in (12) and (13):

$$a_{est} = \frac{1}{2} (a_{1+j_{low}} + a_{j_{high}}) \quad (12)$$

$$\sigma_a = \frac{1}{2} (-a_{1+j_{low}} + a_{j_{high}}) \quad (13)$$

Particularly, the linear regressions in (4) and (5) are performed using the Deming formulation [34] which accounts for error in the independent and dependent variables observations. To each observation, the associated uncertainty is given by the root sum square of the instrumental uncertainty and the statistical uncertainty on the averaging time.

B. Power Curve Analysis

The conventional approach to assess wind turbine performance involves utilizing the bin method for power curve analysis [35]. This method operates under the assumption that, in theory, a wind turbine power curve should manifest as a line on a plane, where the x-axis represents wind speed, and the y-axis denotes the generated power. However, in practice, the power curve is more accurately represented as a scattered distribution of points. This deviation occurs due to various environmental factors, including turbulence, wind veer, and external temperature. Thus, the procedure goes as follows:

- Renormalize the wind speed measurements using (1);
- Group the data per wind speed intervals (the typical choices are 0.5 or 1 m s^{-1} of bin amplitude);
- Compute the average power P_i as in (14) for each i -th bin of wind speed, which will contain N_i measurements:

$$P_i = \frac{1}{N_i} \sum_{j=1}^{N_i} P_{i,j} \quad (14)$$

where $P_{i,j}$ is the j -th measurement of power comprised in the i -th wind speed bin.

- Obtain the average power curve in the (v, P) plane, given by the points (v_i, P_i) .

Given two general data sets D_1 and D_2 at disposal, it is possible to compute two average power curves, given by the sets (v_1, P_1) and (v_2, P_2) with associated frequencies $f_{1,i}$ and $f_{2,i}$ for the various wind speed bins. Therefore, the percentage performance change between the data set D_2 and the data set D_1 can be computed as given in (15):

$$\Delta_{2,1} = \frac{\sum_i f_{2,i} (P_{2,i} - P_{1,i})}{\sum_i f_{1,i} P_{1,i}} \quad (15)$$

In (15), the $f_{2,i}$'s are the frequencies for each i -th wind speed bin in the data set D_2 and $(v_i, P_{1,i})$ and $(v_i, P_{2,i})$ are the observed power curves during D_1 and D_2 respectively. Given that the objective of this work is to compare the behavior of the wind turbine when it is subjected to a static yaw error vs. when it is not, D_2 and D_1 are selected as the $D_{\pm 10}$ and D_0 data set, respectively.

For the sake of clarity, it is crucial to remark that two different wind speed measurements for the x-axis of the power curves have been considered for both D_2 and D_1 , which are the nacelle wind speed v_n and the meteorological mast wind speed v_s . The comparison between the power curves built by considering these two different wind speeds on the one hand reveals the effect of the yaw static error on wind turbine performance, because the meteorological mast wind speed is unaffected by the presence of the yaw error, and on the other hand makes manifest how the power curves constructed with the nacelle wind speed v_n are incoherent, because v_n is affected by the presence of the yaw error.

C. Operation Analysis

Considering the critical insights presented in this work regarding nacelle wind speed measurements, the subsequent proposals aim to identify responses of the wind turbine to

the static yaw error without relying on nacelle wind speed measurements.

In particular, the binning method applied in Section III-B for the power curve analysis can be generalized for whatever couple of variables and subsequently elaborated. For example, this work considers the power-average blade pitch and the power-tower vibrations curves. The former curve is considered because a static yaw error causes non-optimal wind turbine performance. Hence, the power-blade pitch curve is adequate for individuating efficiency losses without employing wind speed measurements because the higher the blade pitch requested for extracting a certain power the higher the wind power which is thrown away and, thus, the lower the efficiency.

On the other hand, the tower vibration curve has been considered to explore the possibility that the presence of the static yaw error is associated with increased vibrations.

For both types of curves, the procedure is the same as outlined in Section III-B. With the data sets at disposal, in this work, the measurements are arranged per power bins of 100 kW from 200 to 1600 kW. For the curves related to the tower vibrations, it should be kept in mind that such measurements are expected to have a vanishing mean. Thus, their absolute value and their standard deviation over the ten-second time interval are analyzed in place of the raw measurements.

Particularly, vibration level parameters $\eta_{abs.vibr}$ and $\eta_{std.vibr}$ are elaborated from the $(P, |\Theta|)$ and (P, σ_Θ) curves (where the standard deviation of the tower vibrations is indicated with σ_Θ) by simply computing the weighted average of the response $|\Theta|$ or σ_Θ , where the weights are the frequencies for the power bins.

IV. EXPERIMENTAL RESULTS

A. Wind Speed Analysis

Fig. 4 and 5 show the results of the wind speed analysis. Particularly, when the yaw error is $+10^\circ$, the wind speed measured by the nacelle anemometer is systematically higher than that measured by the meteorological mast sonic anemometer. In the -10° case, the difference with respect to the 0° case is less pronounced. The different behavior between the $+10^\circ$ and -10° indicates that the results likely depend on the relation between the yaw error and the rotor sense of rotation.

Upon this analysis, the least squares estimates of the coefficients k_{ns} and k_{nc} from the linear models in Equation 4 and 5 are computed and reported in Table II and III. These coefficients describe the linear relation between the meteorological mast wind speed and the nacelle wind speed. Then, a noticeable change in them when the yaw error varies is the symptom that the nacelle wind speed measurements are affected by the yaw error itself. From Table II and III, it is argued that the coefficients largely increase in the $+10^\circ$ case with respect to the 0° , while they decrease slightly in the opposite case -10° . Although basic aerodynamic principles suggest that symmetrical static yaw errors ($\pm 10^\circ$) should have an equal effect on wind turbine performance, in reality, this is not the case. The rotation of the rotor exacerbates (or reduces) the impact of flow acceleration in the vicinity of the nacelle anemometer, resulting in asymmetrical effects.

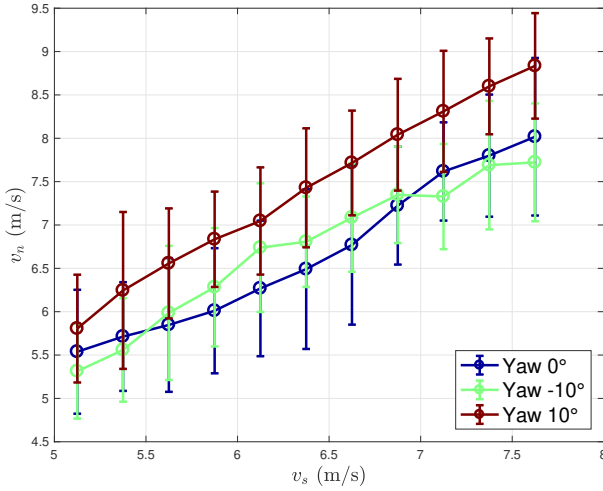


Fig. 4. The average nacelle anemometer wind speed (v_n) per meteorological tower sonic anemometer wind speed (v_s) intervals of 0.25 m s^{-1} . Bins with more than 50 measurements are kept.

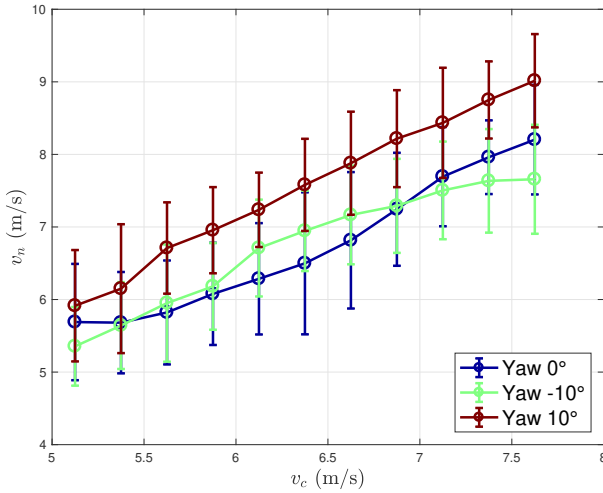


Fig. 5. The average nacelle anemometer wind speed (v_n) per meteorological tower cup anemometer wind speed (v_c) intervals of 0.25 m s^{-1} . Bins with more than 50 measurements are kept.

It is important to remark that the uncertainty analysis conducted with the Deming regression and the Montecarlo simulation shows that the coefficients in the presence of the static yaw error change at least in the order of 6 estimated standard deviations (Table II and III). This gives robustness to the conclusion that the static yaw error alters the relation between meteorological wind speed measurements and nacelle wind speed measurements.

B. Power Curve Analysis

The power curves obtained using the nacelle anemometer are reported in Fig. 6. Particularly, in the case with 10° of static yaw error, the power curve appears largely underperforming, while in the case -10° the power curve appears to be comparable with the 0° case (or even better performing for some wind speed bins) and this is not consistent. This means that the results of [27] about the power curve analysis, as well as those here collected for the 10° case, might be explained

TABLE II

THE LEAST SQUARES ESTIMATES OF k_{ns} , DESCRIBING THE LINEAR RELATION BETWEEN THE SONIC ANEMOMETER METEOROLOGICAL MAST WIND SPEED v_s AND THE NACELLE WIND SPEED v_n , FOR THE VARIOUS VALUES OF THE YAW ERROR.

Data Set	k_{ns}	$\sigma_{k_{ns}}$
D_0	1.0691	0.0004
D_{10}	1.1637	0.0005
D_{-10}	1.0460	0.0010

TABLE III

THE LEAST SQUARES ESTIMATES OF k_{nc} , DESCRIBING THE LINEAR RELATION BETWEEN THE CUP ANEMOMETER METEOROLOGICAL MAST WIND SPEED v_c AND THE NACELLE WIND SPEED v_n , FOR THE VARIOUS VALUES OF THE YAW ERROR.

Data Set	k_{nc}	$\sigma_{k_{nc}}$
D_0	1.0812	0.0005
D_{10}	1.1653	0.0006
D_{-10}	1.0480	0.0010

by the hypothesis that the nacelle wind speed measurement is biased (overestimated) in the presence of the static yaw error. Such effect thus leads to exaggerating the apparent effect of the yaw error on the power curve. This is consistent with the results reported in Table II and III because in the 10° case, the coefficients increase. This means that in the 10° case the measured nacelle wind speed increases for a given average meteorological mast wind speed.

One of the main outcomes of this work is that, when comparing the performance of a wind turbine in two periods in the presence or absence of static yaw error, it is mandatory to employ a reference for environmental conditions that is not affected by the yaw static error. For example, meteorological mast measurements can provide an unbiased reference of the environmental conditions, enabling a more accurate comparison of wind turbine performance. Nevertheless, the power curves reported in Fig. 7 show that it is any case complicated to use as a reference for wind turbine performance analysis a wind speed which is measured around two rotor diameters far from the rotor. Indeed, the shape of the average curves reported in Fig. 7 is qualitatively less regular with respect to the nominal power curve. Anyway, despite this critical point which is comprehensible, the curves in Fig. 7 are coherent, differently with respect to what happens when employing the nacelle wind speed (Fig. 6).

Also the results in Table IV for the performance change between the presence or absence of the yaw error (according to (15)) indicate that the assumption that v_n is unbiased by the presence of static yaw error is implausible. For example, when using the nacelle wind speed measurements to compute the power curves, a static yaw error of -10° is estimated to cause an average performance improvement of +1.7% compared to the 0° case, which is an absurd conclusion. Similarly, the estimated average performance decrease of -20.2% for the -10° degree case is also unrealistic.

Despite the critical points in our analysis due to the dis-

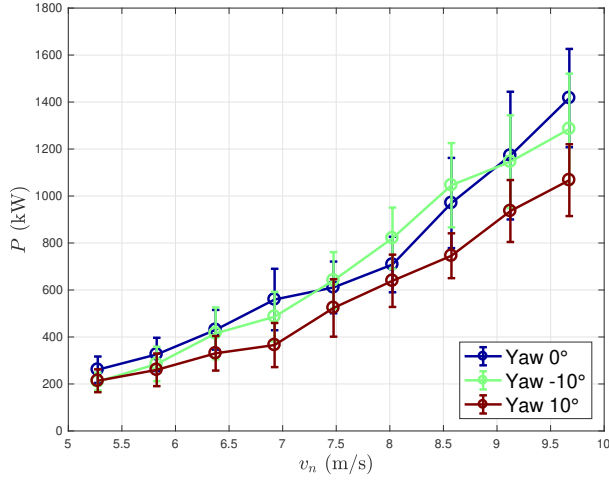


Fig. 6. The average power curve for D_0 , D_{10} and D_{-10} . The nacelle wind speed v_n is used as a reference in the x-axis. Bins with more than 50 measurements are kept.

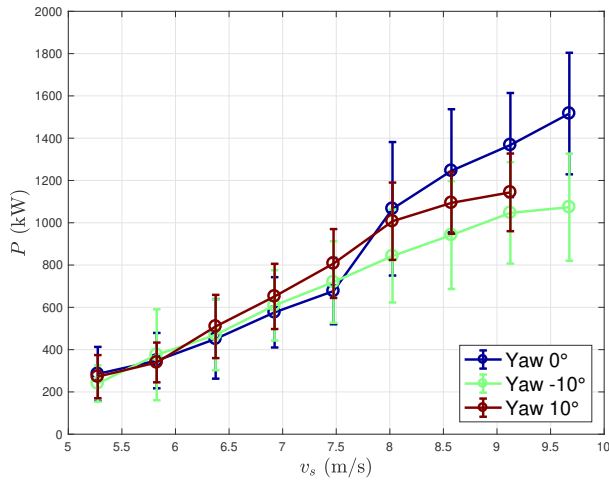


Fig. 7. The average power curve for D_0 , D_{10} and D_{-10} . The meteorological mast sonic anemometer wind speed v_s is used as a reference in the x-axis. Bins with more than 50 measurements are kept.

tance between the meteorological tower and the turbine, the results obtained with v_s are more consistent. Specifically, both positive and negative static yaw errors result in a significant decrease in turbine performance. However, additional data sets are needed to obtain more accurate performance analyses using v_s . It is in any case interesting that the estimates for the $+10^\circ$ and -10° are remarkably different. This means that the effect of the static yaw error on wind turbine performance depends on the relation between the verse of such error and the rotor rotation. Indeed, the \cos^3 law, which is symmetric, is a naive expectation based merely on the fact that, in the presence of a yaw error γ , the component of the wind intensity, which is really perpendicular to the rotor, is $v \cos \gamma$.

C. Operation Analysis

In Fig. 8, the average power-blade pitch curve is reported for the three data sets. It arises that in both yawed cases ($\pm 10^\circ$) there are higher average blade pitches requested to extract a

TABLE IV
THE RESULTS FOR Δ ((15)).

Wind Speed	Δ_{10}	Δ_{-10}
v_n	-20.2%	+1.7%
v_s	-13.4%	-7.2%

certain power, with respect to what happens in the 0° of yaw error case. This phenomenon has to be interpreted with attention. Given a particular model of a wind turbine, the power-blade pitch curve should be unique and should correspond to the operation under the highest possible efficiency, given the rotor design. If two different power-blade pitch curves are observed for a wind turbine (under different conditions, for example in the presence of the static yaw error), if the blade pitch for a certain extracted power is higher, it means that more incoming wind power has been thrown away and thus more incoming wind power was needed for extracting that power. Thus, the ratio between the extracted power and the incoming power is lower, meaning lower efficiency and thus an under-performance. This means that the under-performance associated with the operation under static yaw error can be detected also without using nacelle wind speed measurements. It is noticeable that higher blade pitches are observed for the $+10^\circ$ case with respect to the -10° case, which means a more severe average under-performance. This is a further confirmation that the \pm behavior is not symmetric and that the results collected in Table IV when using the meteorological mast wind speed reference are plausible. Another interesting observation is that the variability of the blade pitch is also higher for the $+10^\circ$ case.

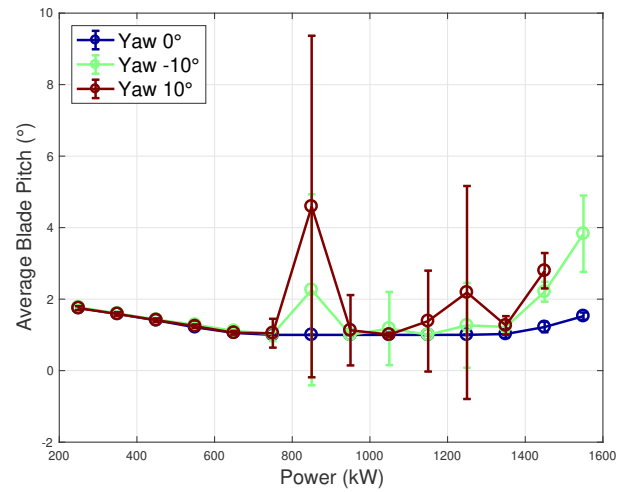


Fig. 8. The average power - blade pitch curve for D_0 , D_{10} and D_{-10} cases.

In Table V, the vibration level parameters formulated in Section III-C are reported for the various cases. An increase is visible for the yawed cases, which is more evident in the 10° with respect to the -10° case. From this analysis, it can be argued that the presence of a static yaw error can be detected also by analyzing the mechanical response of the wind turbine tower.

TABLE V
THE RESULTS FOR VIBRATION LEVEL PARAMETERS η (m s^{-2}).

η	D_0	D_{10}	D_{-10}
$\eta_{abs.vibr}$	0.017	0.021	0.019
$\eta_{std.vibr}$	0.067	0.078	0.071

D. Discussion

Several considerations can be drawn from the above results. The pros and cons of each proposed method and a state-of-the-art method (power curve analysis without critical revision of the nacelle anemometer measurements) are summarized in Table VI. Particularly, it emerges that the analysis of the change in the nacelle wind speed measurements has the fundamental pro of being directly related to the presence of the static yaw error, differently with respect to all the other methods. Indeed, there can be other root causes of a change in the power curve, of an increase in the tower vibrations, and of a change in the power-blade pitch curve, as a blade pitch unbalanced (which instead is not expected to affect the nacelle wind speed measurements). Nevertheless, the method based on the wind speed analysis is more demanding from the point of view of requested data, in that it needs a reference for meteorological conditions that is unaffected by the presence of the static yaw error (meteorological mast data, in the case of this work). Such a drawback can be circumvented if the wind turbine is equipped with two identical nacelle anemometers.

A future direction of this work which is currently under investigation regards an appropriate modification of the flow equilibrium analysis conducted in [30], which is possible when two nacelle anemometers are present. It should be noted that the availability of two nacelle anemometers is the standard for multi-MW wind turbines, then this request is not so demanding. In particular, such measurements could be employed also for estimating the amount of static yaw error. Furthermore, the results of this work could stimulate developments in high-fidelity simulations of the flow across yawed rotors and of the dynamic response (operational and mechanical) of the wind turbines in yawed conditions [36].

Another relevant aspect is the challenge in quantifying the amplitude of the static yaw error, which is a common limitation of the state-of-the-art methods shown in Table VI. However, this does not constitute a severe limitation for the scientific and practical purposes of this work. Actually, from a scientific point of view, the objective of this work was to highlight phenomena relatable to the presence of the static yaw error, which is overlooked in the literature, and this has been possible also with one nacelle anemometer available. From a practical point of view, the type of results collected with the wind speed analysis of this work identifies a wind turbine suspected of being affected by a static yaw error. This kind of information can support the decision maker in investing in upwind sensors like LiDARs. Future work on two nacelle anemometers will likely provide methods based solely on SCADA data which can be used for the correction of the static yaw error without installing additional costly sensors, like LiDARs.

TABLE VI
SUMMARY OF THE PROS AND CONS OF THE VARIOUS METHODS FOR STATIC YAW ERROR DIAGNOSIS.

Method	Pro	Con
Wind speed analysis	It can be put in direct relation with the yaw error.	It requires a met-mast or two nacelle anemometers.
Blade pitch analysis	It requires a minimal amount of SCADA-collected measurements (power and blade pitch)	It is difficult to establish a causal relation with the presence of the yaw error.
Vibration analysis	It requires a minimal amount of SCADA-collected measurements (power and tower vibrations)	It is difficult to establish a causal relation with the presence of the yaw error.
Naive power curve analysis	It requires a minimal amount of SCADA-collected measurements (power and nacelle wind speed)	Lack of coherence and it is difficult to establish a causal relation with the presence of the yaw error.

Finally, it is worth noticing that for completeness the analysis of this work was conducted by employing the measurements from the sonic and cup anemometers of the meteorological mast. Yet, the conclusions are similar and it can be argued that, from this point of view, wind turbine practitioners can be guided merely by cost considerations because there is no loss in employing solely a sonic or solely a cup anemometer at the meteorological mast.

V. CONCLUSION

Wind energy represents a promising alternative to traditional fossil-based energy sources. Hence, it is crucial to increase the efficiency of the conversion process from wind to electrical energy. Unfortunately, static errors as the yaw alignment error, significantly contribute to under-performance, necessitating thorough identification. Despite its crucial importance, the literature has generally overlooked static errors and lacked a comprehensive and coherent characterization of their observable effects on wind turbine operation. Addressing this research gap, this manuscript presented an investigation based on controlled experiments, utilizing a unique experimental test setup at the Eolos Wind Research Station which allowed to deliberately set a utility-scale wind turbine to operate subjected to several values of static yaw error. Key findings include a pipeline for detecting the systematic alteration in nacelle wind speed measurements in the presence of a static yaw error, which is an aspect overlooked in the literature that invalidates most of the state-of-the-art methods, like the power curve analysis. Thus, the results of this work should stimulate a critical revision of the methods currently employed for the diagnosis of the static yaw error based on SCADA data analysis. Finally, the study highlights that, in the presence of the static yaw error, an increased blade pitch, along with heightened levels of tower vibration, can be detected. Further research on the subject should thus take into account that the most straightforward way to ascertain the presence of a wind turbine static yaw error is by individuating a change in

the nacelle wind speed measurements. Such measurements are affected by the presence of the error but are not regulated by the control, differently with respect to what happens with, for example, the power or the rotational speed.

The methodology developed in this study thus, by making explicit experimental evidences associated to the presence of the static yaw error, paves the way for more effective and easier diagnostic techniques for wind turbine yaw errors, potentially revolutionizing data-driven condition monitoring and maintenance strategies.

REFERENCES

- [1] Q. Wang, Z. Dong, R. Li, and L. Wang, "Renewable energy and economic growth: New insight from country risks," *Energy*, vol. 238, p. 122018, 2022.
- [2] B. Xu, "Exploring the sustainable growth pathway of wind power in china: Using the semiparametric regression model," *Energy Policy*, vol. 183, p. 113845, 2023.
- [3] U. Elosegui, I. Egana, A. Ulazia, and G. Ibarra-Berastegi, "Pitch angle misalignment correction based on benchmarking and laser scanner measurement in wind farms," *Energies*, vol. 11, no. 12, p. 3357, 2018.
- [4] F. Castellani, A. Eltayesh, M. Becchetti, and A. Segalini, "Aerodynamic analysis of a wind-turbine rotor affected by pitch unbalance," *Energies*, vol. 14, no. 3, p. 745, 2021.
- [5] D. Astolfi, R. Pandit, A. Lombardi, and L. Terzi, "Diagnosis of wind turbine systematic yaw error through nacelle anemometer measurement analysis," *Sustainable Energy, Grids and Networks*, vol. 34, p. 101071, 2023.
- [6] D. Astolfi, F. Castellani, M. Becchetti, A. Lombardi, and L. Terzi, "Wind turbine systematic yaw error: Operation data analysis techniques for detecting it and assessing its performance impact," *Energies*, vol. 13, no. 9, p. 2351, 2020.
- [7] R. Bakhshi and P. Sandborn, "The effect of yaw error on the reliability of wind turbine blades," in *Energy Sustainability*, vol. 50220. American Society of Mechanical Engineers, 2016, p. V001T14A001.
- [8] F. Bernardoni, M. A. Rotea, and S. Leonardi, "Impact of yaw misalignment on turbine loads in the presence of wind farm blockage," *Wind Energy*, 2024.
- [9] L. Yuan, H. Meng, Y. Liu, K. Long, G. Wu, and X. Liu, "Research on the aerodynamic characteristics of wind turbine under coupled pitching motion and yaw error," 2023.
- [10] Y. Pei, Z. Qian, B. Jing, D. Kang, and L. Zhang, "Data-driven method for wind turbine yaw angle sensor zero-point shifting fault detection," *Energies*, vol. 11, no. 3, p. 553, 2018.
- [11] J. Yang, L. Wang, D. Song, C. Huang, L. Huang, and J. Wang, "Incorporating environmental impacts into zero-point shifting diagnosis of wind turbines yaw angle," *Energy*, vol. 238, p. 121762, 2022.
- [12] A. Rott, L. Höning, P. Hulsmann, L. J. Lukassen, C. Moldenhauer, and M. Kühn, "Wind vane correction during yaw misalignment for horizontal axis wind turbines," *Wind Energy Science Discussions*, vol. 2023, pp. 1–28, 2023.
- [13] D. Choi, W. Shin, K. Ko, and W. Rhee, "Static and dynamic yaw misalignments of wind turbines and machine learning based correction methods using lidar data," *IEEE Transactions on Sustainable Energy*, vol. 10, no. 2, pp. 971–982, 2018.
- [14] L. Zhang and Q. Yang, "A method for yaw error alignment of wind turbine based on lidar," *IEEE Access*, vol. 8, pp. 25 052–25 059, 2020.
- [15] T. F. Pedersen, G. Demurtas, and F. Zahle, "Calibration of a spinner anemometer for yaw misalignment measurements," *Wind Energy*, vol. 18, no. 11, pp. 1933–1952, 2015.
- [16] G. Demurtas, T. F. Pedersen, and F. Zahle, "Calibration of a spinner anemometer for wind speed measurements," *Wind Energy*, vol. 19, no. 11, pp. 2003–2021, 2016.
- [17] R. Bakhshi and P. Sandborn, "Analysis of wind turbine capacity factor improvement by correcting yaw error using lidar," in *ASME International Mechanical Engineering Congress and Exposition*, vol. 58417. American Society of Mechanical Engineers, 2017, p. V006T08A092.
- [18] —, "Maximizing the returns of lidar systems in wind farms for yaw error correction applications," *Wind Energy*, vol. 23, no. 6, pp. 1408–1421, 2020.
- [19] Y. Wang, Q. Hu, L. Li, A. M. Foley, and D. Srinivasan, "Approaches to wind power curve modeling: A review and discussion," *Renewable and Sustainable Energy Reviews*, vol. 116, p. 109422, 2019.
- [20] Y. Ding, *Data science for wind energy*. CRC Press, 2019.
- [21] A. Clifton, S. Barber, A. Bray, P. Enevoldsen, J. Fields, A. M. Sempreviva, L. Williams, J. Quick, M. Purdue, P. Totaro *et al.*, "Grand challenges in the digitalisation of wind energy," *Wind Energy Science*, vol. 8, no. 6, pp. 947–974, 2023.
- [22] B. Jing, Z. Qian, Y. Pei, L. Zhang, and T. Yang, "Improving wind turbine efficiency through detection and calibration of yaw misalignment," *Renewable Energy*, vol. 160, pp. 1217–1227, 2020.
- [23] Y. Bao, Q. Yang, S. Li, K. Miao, and Y. Sun, "A data-driven approach for identification and compensation of wind turbine inherent yaw misalignment," in *2018 33rd Youth Academic Annual Conference of Chinese Association of Automation (YAC)*. IEEE, 2018, pp. 961–966.
- [24] Y. Bao, Q. Yang, L. Fu, Q. Chen, C. Cheng, and Y. Sun, "Identification of yaw error inherent misalignment for wind turbine based on scada data: A data mining approach," in *2019 12th Asian Control Conference (ASCC)*. IEEE, 2019, pp. 1095–1100.
- [25] Y. Bao and Q. Yang, "A data-mining compensation approach for yaw misalignment on wind turbine," *IEEE Transactions on Industrial Informatics*, vol. 17, no. 12, pp. 8154–8164, 2021.
- [26] R. Pandit, D. Infield, and T. Dodwell, "Operational variables for improving industrial wind turbine yaw misalignment early fault detection capabilities using data-driven techniques," *IEEE Transactions on Instrumentation and Measurement*, vol. 70, pp. 1–8, 2021.
- [27] C. Qu, Z. Lin, P. Chen, J. Liu, Z. Chen, and Z. Xie, "An improved data-driven methodology and field-test verification of yaw misalignment calibration on wind turbines," *Energy Conversion and Management*, vol. 266, p. 115786, 2022.
- [28] L. Gao and J. Hong, "Data-driven yaw misalignment correction for utility-scale wind turbines," *Journal of Renewable and Sustainable Energy*, vol. 13, no. 6, p. 063302, 2021.
- [29] K. S. Heck, H. M. Johlas, and M. F. Howland, "Modelling the induction, thrust and power of a yaw-misaligned actuator disk," *Journal of Fluid Mechanics*, vol. 959, p. A9, 2023.
- [30] N. Mittelmeier and M. Kühn, "Determination of optimal wind turbine alignment into the wind and detection of alignment changes with scada data," *Wind Energy Science*, vol. 3, no. 1, pp. 395–408, 2018.
- [31] D. Astolfi, L. Gao, R. Pandit, and J. Hong, "Experimental analysis of the effect of static yaw error on wind turbine nacelle anemometer measurements," in *2023 IEEE International Conference on Environment and Electrical Engineering and 2023 IEEE Industrial and Commercial Power Systems Europe (EEEIC/I&CPS Europe)*. IEEE, 2023, pp. 1–6.
- [32] L. Gao, S. Yang, A. Abraham, and J. Hong, "Effects of inflow turbulence on structural response of wind turbine blades," *Journal of wind engineering and industrial aerodynamics*, vol. 199, p. 104137, 2020.
- [33] L. Gao, B. Li, and J. Hong, "Effect of wind veer on wind turbine power generation," *Physics of Fluids*, vol. 33, no. 1, p. 015101, 2021.
- [34] S. Saraçlı and A. H. Türkan, "A comparison of linear regression techniques in method comparison studies," *Journal of Statistical Computation and Simulation*, vol. 83, no. 10, pp. 1890–1899, 2013.
- [35] IEC, "Power performance measurements of electricity producing wind turbines," International Electrotechnical Commission, Geneva, Switzerland, Tech. Rep. 61400–12, 2005.
- [36] G. M. Starke, C. Meneveau, J. R. King, and D. F. Gayme, "A dynamic model of wind turbine yaw for active farm control," *Wind Energy*, 2023.



Davide Astolfi (M'23) received the B.S., M.S. and Ph.D. degree in Physics at the University of Perugia (Italy) and the Ph.D. degree in Industrial and Information Engineering at the University of Perugia. He is currently an Assistant Professor in Electrical Systems for Energy at the University of Brescia. His research interests include wind turbine technology, data analysis and artificial intelligence applications for renewable energy, supervisory control and data acquisition, wind power forecasting, electric vehicles charging systems. He serves as an associate editor for several international journals.



Fabrizio De Caro (IEEE Member) (M'14) was born in Benevento, Italy, in 1992. He received the B.Sc and M.Sc degrees in energy engineering and the Ph.D. degree in information technologies for engineering from the University of Sannio, (UniSannio), Benevento, Italy in 2014, 2016, and 2020, respectively. He is a Postdoc Researcher with the S.I.S.T.E.M.I. group in the Industrial Engineering Department, University of Salerno (UniSa), Fisciano, Italy, and a scientific collaborator with the Machine Learning Group (MLG), Université Libre

de Bruxelles, Belgium. His research interests include effective renewable energy sources integration in smart grids, wind power forecasting, artificial intelligence in power systems, decision-making tools in the presence of uncertainty, electricity markets, and resilience of power systems. He is an IEEE member since 2014 and serves as Associate Editor and reviewer for several international journals.



Alfredo Vaccaro (M'01–SM'10) received the M.Sc. (Hons.) degree in electronic engineering from the University of Salerno, Salerno, Italy, and the Ph.D. degree in electrical and computer engineering from the University of Waterloo, Waterloo, ON, Canada. From 1999 to 2002, he was an Assistant Researcher with the Department of Electrical and Electronic Engineering, University of Salerno. From March 2002 to October 2015, he was an Assistant Professor of electric power systems with the Department of Engineering, University of Sannio, Benevento, Italy,

where he is currently a Full Professor of electrical power systems. His research interests include soft computing and interval-based method applied to power system analysis, and advanced control architectures for diagnostic and protection of distribution networks. He is a Senior Member IEEE and an Associate Editor for the IEEE Transaction on Power Systems, IEEE Transaction on Smart Grids.



Marco Pasetti (M'19) received the M.Sc. degree in industrial engineering and the Ph.D. degree in mechanical engineering from the University of Brescia, Brescia, Italy, in 2008 and 2013, respectively. He is currently Assistant Professor of electrical energy systems with the Department of Information Engineering, University of Brescia. His current research interests include energy systems, distributed generation, renewable energy sources, photovoltaics, energy storage, demand-side management, electric vehicles charging systems, energy management systems,

supervisory control and data acquisition, and smart grids.



Linyue Gao is an Assistant Professor of Mechanical Engineering at the University of Colorado, where her research focuses on developing and optimizing advanced flow diagnostics and instrumentations and applying our flow imaging knowledge and skills to reveal fundamental principles in thermal fluid and energy systems. Dr. Gao received her B.S. (2013) and M.S. (2016) in Renewable Energy from North China Electric Power University and Ph.D. (2019) in Aerospace Engineering from Iowa State University. Prior to her current position, she was a Postdoctoral

Associate (2019-2021) at the St. Anthony Falls Laboratory at the University of Minnesota and an Assistant Professor (2021-2022) at California State University. Dr. Gao has authored more than 40 journal articles and conference papers and has been honored with the China National Scholarship, Brown Graduate Fellowship, and Renewable Energy Commercialization Fellowship.



Jiarong Hong received the B.S. degree from the University of Science and Technology of China, Hefei, China, in 2005, and the M.S. and Ph.D. degrees from Johns Hopkins University, Baltimore, MD, USA, in 2008 and 2011, respectively. He is currently a Professor with the Mechanical Engineering Department and the Saint Anthony Falls Laboratory, University of Minnesota, Minneapolis, MN, USA. His research interests include the development of novel imaging techniques for analyzing flow and particle transport across a broad range of disciplines.

Dr. Hong was a recipient of the National Science Foundation CAREER Award and the Office of Naval Research Young Investigator Award.



Ravi Pandit received the bachelor's degree from Jadavpur University, Kolkata, India, in 2009, the master's degree from the Indian Institute of Technology Kharagpur, Kharagpur, India, in 2011, and the Ph.D. degree from the University of Strathclyde, Glasgow, U.K., in 2019. He is currently a Lecturer of instrumentation and AI with the Centre for Life-Cycle Engineering and Management, School of Aerospace, Transport and Manufacturing, Cranfield University, Cranfield, U.K. From 2011 to 2016, he was an Assistant Professor with Jadavpur University

and the Vellore Institute of Technology, Vellore, India. His research interests include data-driven applications on offshore wind including condition monitoring, predictive maintenance, forecasting and prediction, and SCADA data statistical analysis. He has more than five years of direct research experience in his research areas.

Investigation of wind turbine static yaw error based on utility-scale controlled experiments

Astolfi, Davide

2024-05-08

Attribution-NonCommercial 4.0 International

Astolfi D, De Caro F, Pasetti M, et al., (2024) Investigation of wind turbine static yaw error based on utility-scale controlled experiments. IEEE Transactions on Industry Applications. Available online 08 May 2024

<https://doi.org/10.1109/TIA.2024.3397956>

Downloaded from CERES Research Repository, Cranfield University